BJP British Journal of Pharmacology

DOI:10.1111/bph.12044
www.brjpharmacol.org

RESEARCH PAPER

Ca^{2+} sparks promote myogenic tone in retinal arterioles

J Kur†, P Bankhead‡, CN Scholfield§, TM Curtis* and JG McGeown*

Centre for Vision and Vascular Science, School of Medicine, Dentistry and Biomedical Sciences, Queen's University Belfast, Belfast, UK

Correspondence
Professor Graham McGeown, CVVS (ICS(A)), Queen's University Belfast, Royal Victoria Hospital Campus, Grosvenor Road, Belfast BT12 6BA, UK.
E-mail: g.mcgeown@qub.ac.uk

*Contributed equally as senior authors.
†Present address: Department of Neuroscience, University of Minnesota, Minneapolis, US.
‡Present address: Nikon Imaging Center, University of Heidelberg, Germany.
§Present address: Faculty of Pharmaceutical Sciences, Naresuan University, Phitsanulok, Thailand.

Source of funding: Fight for Sight UK, British Heart Foundation.

Keywords
microcirculation; arterioles; Ca^{2+} sparks; Ca^{2+} oscillations; vascular smooth muscle; myogenic tone

Received
25 May 2012
Revised
30 October 2012
Accepted
30 October 2012

BACKGROUND AND PURPOSE

Ca^{2+} imaging reveals subcellular Ca^{2+} sparks and global Ca^{2+} waves/oscillations in vascular smooth muscle. It is well established that Ca^{2+} sparks can relax arteries, but we have previously reported that sparks can summate to generate Ca^{2+} waves/oscillations in unpressurized retinal arterioles, leading to constriction. We have extended these studies to test the functional significance of Ca^{2+} sparks in the generation of myogenic tone in pressurized arterioles.

EXPERIMENTAL APPROACH

Isolated retinal arterioles (25–40 μm external diameter) were pressurized to 70 mmHg, leading to active constriction. Ca^{2+} signals were imaged from arteriolar smooth muscle in the same vessels using Fluo4 and confocal laser microscopy.

KEY RESULTS

Tone development was associated with an increased frequency of Ca^{2+} sparks and oscillations. Vasomotion was observed in 40% of arterioles and was associated with synchronization of Ca^{2+} oscillations, quantifiable as an increased cross-correlation coefficient. Inhibition of Ca^{2+} sparks with ryanodine, tetracaine, cyclopiazonic acid or nimodipine, or following removal of extracellular Ca^{2+}, resulted in arteriolar relaxation. Cyclopiazonic acid-induced dilatation was associated with decreased Ca^{2+} sparks and oscillations but with a sustained rise in the mean global cytoplasmic $[Ca^{2+}]$ ($[Ca^{2+}]_c$), as measured using Fura2 and microfluorimetry.

CONCLUSIONS AND IMPLICATIONS

This study provides direct evidence that Ca^{2+} sparks can play an excitatory role in pressurized arterioles, promoting myogenic tone. This contrasts with the generally accepted model in which sparks promote relaxation of vascular smooth muscle. Changes in vessel tone in the presence of cyclopiazonic acid correlated more closely with changes in spark and oscillation frequency than global $[Ca^{2+}]_c$, underlining the importance of frequency-modulated signalling in vascular smooth muscle.

Abbreviations

BK, large conductance Ca^{2+}-sensitive K^+ channel; $[Ca^{2+}]_c$, cytosolic Ca^{2+} concentration; CCC, cross-correlation coefficient; CPA, cyclopiazonic acid; FDHM, full duration half-maximum; SR, sarcoplasmic reticulum

Introduction

Regulation of arteriolar tone plays a crucial role both in control of arterial blood pressure and modulation of tissue blood flow to meet changes in metabolic need (Secomb, 2008; Martinez-Lemus, 2012). As in other muscle types, Ca^{2+} signalling within the vascular myocytes is crucial to excitation–contraction coupling, allowing a wide range of chemical, mechanical and electrical stimuli to be transduced into an appropriate mechanical response (Marchand *et al.*, 2012). Microfluorimetry techniques consistently demonstrate that vascular smooth muscle contraction, the cellular correlate of vasoconstriction, is preceded by an increase in the average cytoplasmic $[Ca^{2+}]$ ($[Ca^{2+}]_c$) (Sato *et al.*, 1988). The introduction of high-speed Ca^{2+} imaging, however, revealed that changes in $[Ca^{2+}]_c$ are not as homogeneous at the cell level as suggested by whole vessel recordings. Apparently tonic increases in the average $[Ca^{2+}]_c$ within the muscle of a vessel segment may actually result from unsychronized phasic $[Ca^{2+}]_c$ signals within adjacent myocytes (Iino *et al.*, 1994; McGeown, 2010). These phasic signals have been categorized into Ca^{2+} sparks, waves and oscillations, based on their spatiotemporal characteristics.

Both Ca^{2+} waves and oscillations involve an increase in global $[Ca^{2+}]_c$, which either propagates along the cell length (waves) or occurs more or less synchronously throughout (oscillations). These signals lead to myocyte contraction and vascular constriction. Studies in vascular smooth muscle suggest that nerve- and agonist-induced contractions reflect an increased frequency of Ca^{2+} oscillations, rather than a tonic rise in global $[Ca^{2+}]_c$ (Iino *et al.*, 1994; Perez and Sanderson, 2005). Ca^{2+} sparks, in contrast, are brief and highly localized subcellular Ca^{2+} release events that may achieve relatively high Ca^{2+} concentrations within a local microdomain but do not, themselves, propagate through the rest of the cytoplasm (Zhuge *et al.*, 2004). Ca^{2+} sparks reflect spontaneous release from the sarcoplasmic reticulum via ryanodine receptors (RyRs) and act as building blocks in the generation of Ca^{2+} transients during cardiac excitation–contraction coupling (Cheng *et al.*, 1993). Paradoxically, however, their role in vascular myocytes and other smooth muscle is generally believed to be inhibitory (Nelson *et al.*, 1995; Burdyga and Wray, 2005). Sparks can activate large conductance, Ca^{2+}-sensitive K^+ (BK) channels in the smooth muscle cell membrane, causing hyperpolarization and deactivation of voltage-sensitive Ca^{2+} channels. The consequent reduction in global cytosolic $[Ca^{2+}]_c$ leads to muscle relaxation and vasodilatation (Cheng and Lederer, 2008). This mechanism has been shown to play an important role in arterial dilator responses to agents such as NO (Mandala *et al.*, 2007). More recently, similar observations have been reported in pressurized cerebral arterioles, suggesting sparks can play an inhibitory role in microvessels as well (Dabertrand *et al.*, 2012; Liang *et al.*, 2012). It is important to note, however, that considerable heterogeneity is likely to be seen within different vascular beds and even different regions of the same bed. For example, Ca^{2+} sparks appear to play a classical inhibitory role within skeletal muscle feed arteries, but no sparks are observed within their downstream arterioles. Inhibition of ryanodine receptors, which constricts pressurized feed arteries, has no effect on myogenic tone in the related arterioles (Westcott and Jackson, 2011; Westcott *et al.*, 2012).

Although a vasodilatory action for sparks is widely reported, it is not universal. Ca^{2+} imaging of isolated portal vein myocytes has revealed spark 'frequent discharge sites' that also act as sites for initiation of global Ca^{2+} waves, resulting in cell contraction (Bolton and Gordienko, 1998; Gordienko *et al.*, 2001). Stretching isolated smooth muscle from renal afferent arterioles stimulates spark activity and triggers global Ca^{2+} release and contraction via an integrin-dependent mechanism (Balasubramanian *et al.*, 2007). Previous results from our laboratory also suggest that Ca^{2+} sparks can summate to generate prolonged Ca^{2+} oscillations associated with muscle contraction in retinal arterioles, suggesting an excitatory role (Tumelty *et al.*, 2007). Consistent with this, sparks and waves/oscillations are also increased in frequency in response to vasoconstricting agonists (Jeffries *et al.*, 2010; Tumelty *et al.*, 2011). However, although these experiments were carried out on intact arteriole segments, rather than isolated myocytes, the arterioles were not pressurized and did not demonstrate physiological myogenic tone (Hill *et al.*, 2007). We have now developed a preparation in which changes in vessel diameter and Ca^{2+} signalling can be recorded from the same arteriole before and after development of myogenic tone and following pharmacological interventions that modify spark activity. Our results lead us to conclude that Ca^{2+} sparks play an excitatory role in retinal arteriolar smooth muscle, promoting vascular constriction in response to stretch. To the best of our knowledge, this is the first demonstration that Ca^{2+} sparks can play an excitatory role in the smooth muscle of a pressurized vessel under conditions of myogenic tone. We also show that arteriolar tone correlates with spark and oscillation frequency, rather than the tissue averaged $[Ca^{2+}]_c$, under conditions in which these diverge, underlining the importance of phasic signalling in the control of vascular smooth muscle contraction.

Methods

Arteriole preparation

Male Sprague–Dawley rats (8–12 weeks of age; 200–250 g) were killed using i.p. sodium pentobarbital (300 mg·kg^{-1} body weight) in accordance with UK legal and local institutional requirements. Retinas were placed in low Ca^{2+} Hanks' solution [in mmol·L^{-1}: 140, NaCl; 6, KCl; 5, D-glucose; 0.1, $CaCl_2$; 1.3, $MgCl_2$; 10, HEPES (pH 7.4 with NaOH)] and mechanically

triturated using a Pasteur pipette, as previously described (Curtis *et al.*, 2004). The resulting suspension was centrifuged at 1200× *g* for 1 min, and the supernatant was removed. The tissue was pipetted into a recording bath mounted on an inverted microscope. Arteriole segments (25–40 μm outside diameter and 400–4000 μm long) devoid of neuropile or perivascular astrocytes were easily identified by the continuous monolayer of smooth muscle cells. All studies involving animals are reported in accordance with the ARRIVE guidelines for reporting experiments involving animals (Kilkenny *et al.*, 2010; McGrath *et al.*, 2010). All experiments were carried out at 37°C, and all drugs were purchased from Sigma (UK) and applied to the outside of the arterioles in pre-warmed bath solution.

Pressure myography

The development of myogenic tone was assessed using pressure myography, as previously described (McGahon *et al.*, 2007a). A tungsten wire slip (75 × 2000 μm) was laid on the arteriole, anchoring and occluding one end. The vessel was then superfused with Ca^{2+}-free Hanks' [in mmol·L^{-1}: 140, NaCl; 6, KCl; 5, D-glucose; 1.3, $MgCl_2$; 10, HEPES (pH 7.4 with NaOH)] at 37°C. The open end was cannulated using a glass micropipette (tip diameters 3–10 μm) filled with Ca^{2+}-free medium, using a patch electrode holder and micromanipulator. The pipette was connected to a pressure transducer and water manometer. Following introduction of the pipette, the vessel was superfused with Hanks' solution containing 2 mmol·L^{-1} Ca^{2+} for 15 min, allowing the pipette to seal to the inner vessel wall. The arteriole was then inflated to the desired pressure. Preparations were leak-tested by observing a small air bubble introduced into the cannula connecting the pipette to the manometer. In the absence of leakage around the pipette or through the arteriolar wall, this bubble remained relative static at fixed high pressure. The fact that a range of interventions led to reversible vasodilatation following development of tone (Figures 1 and 3) indicates that the constrictions seen reflected myogenic vascular contraction, rather than mechanical artefacts due to fluid leakage and loss of pressure. A section of vessel at least 150 μm away from the cannula was viewed under a ×40 (numerical aperture = 0.6) objective focused in the plane of maximal vessel diameter. Bright-field images were captured at 2 s intervals using a MCN-B013-U USB camera aligned with the long axis of the arteriole. Acquisition and analysis were carried out using custom software implemented in Delphi. The outer vessel edge was first identified manually and then tracked automatically within a specified region of interest (ROI). The average external diameter for this ROI was determined for each image, and the output was converted to micrometers using a calibration graticule image.

Subcellular Ca^{2+} imaging

In experiments in which mechanical responses and changes in Ca^{2+} sparks and oscillations were recorded from the same vessels, vascular fragments were pre-incubated with the fluorescent Ca^{2+} indicator Fluo-4AM (10 μmol·L^{-1} for 2 h). The image plane was focussed on the smooth muscle layer lying on the bottom of the recording chamber, rather than the plane of maximal diameter as for pressure myography. Ca^{2+} images were recorded from cannulated arterioles before pressurization. Diameter recordings were then made as described above during pressurization and the development of tone, followed by Ca^{2+} imaging for the same vessel in the new steady state. Myocytes were imaged with a Bio-Rad Radiance 2100 laser scanning confocal microscope using an ×60 oil-immersion objective (N.A. 1.4). Fluo4 was excited at 488 nm, and the emitted light band-pass filtered (530–560 nm) prior to measurement. Fluorescence changes were recorded in line-scan mode along a scan-line orientated parallel to the long axis of the arteriole (i.e. transversely across the short axis of the smooth muscle cells), with a scan rate of 500 scans·s^{-1}. Background fluorescence was measured from a peripheral area in the captured image, distant from the outer edge of the arteriole. Background corrected fluorescence (F) was normalized to the basal fluorescence at any given site (F_0) and changes in F/F_0 interpreted as local changes in $[Ca^{2+}]_c$. Ca^{2+} imaging was carried out in each vessel prior to pressurization and when steady-state myogenic tone had developed following pressurization.

$[Ca^{2+}]_c$ microfluorimetry

In experiments in which changes in global $[Ca^{2+}]_c$ were recorded, arteriolar segments were first incubated with 5 μmol·L^{-1} Fura2-AM for 2 h. This exclusively loads the smooth muscle layer (Scholfield and Curtis, 2000). They were then washed and superfused with Hanks' solution at 37°C in a perfusion bath mounted on the stage of an inverted microscope and cannulated as described above. The vessel was imaged using a ×40 objective (N.A. 0.6). Fura2 fluorescence was excited alternately with 340 nm (F_{340}) and 380 nm (F_{380}) light from a dual monochromator (5 nm bandwidth) using a light chopper (Cairn Research Ltd, Faversham, UK). Emitted fluorescence was collected from an arteriole segment approximately 50 μm in length. Given that the arterioles are surrounded by a smooth muscle monolayer with an average myocyte width of 5 μm, this equates to approximately 10 cells. Light was directed through the side port of the microscope, filtered (510 nm) and detected (5 ratios per second) using a photomultiplier tube (PMT) in photon counting mode. Acquisition and data analysis were controlled using Acquisition Engine (Cairn) software (V1.1.5). At the end of each protocol, the preparation was superfused with a nominally Ca^{2+}-free solution containing 5 mM $MnCl_2$ to quench all free Fura2 fluorescence. The residual fluorescence at each excitation wavelength was subtracted from the absolute counts to correct for background. These corrected counts were then used to calculate the fluorescence ratio ($R = F_{340}/F_{380}$), which was converted to Ca^{2+} concentration using the equation:

$$[Ca^{2+}] = K_d \times \beta \times (R - R_{min})/(R_{max} - R) \quad \text{(Grynkiewicz } \textit{et al.}\text{, 1985)}$$

The following constant values were used: $R_{max} = 1.5$, $R_{min} = 0.2$, $\beta = 2.1$ and $K_d = 250$ nM (see Scholfield and Curtis, 2000). Changes in arteriolar diameter were simultaneously recorded using bright field illumination through a 680 nm long-pass filter to eliminate crosstalk with Fura2 fluorescence. The resulting image was reflected into an infrared camera using a short-pass dichroic mirror in the light path to the PMT.

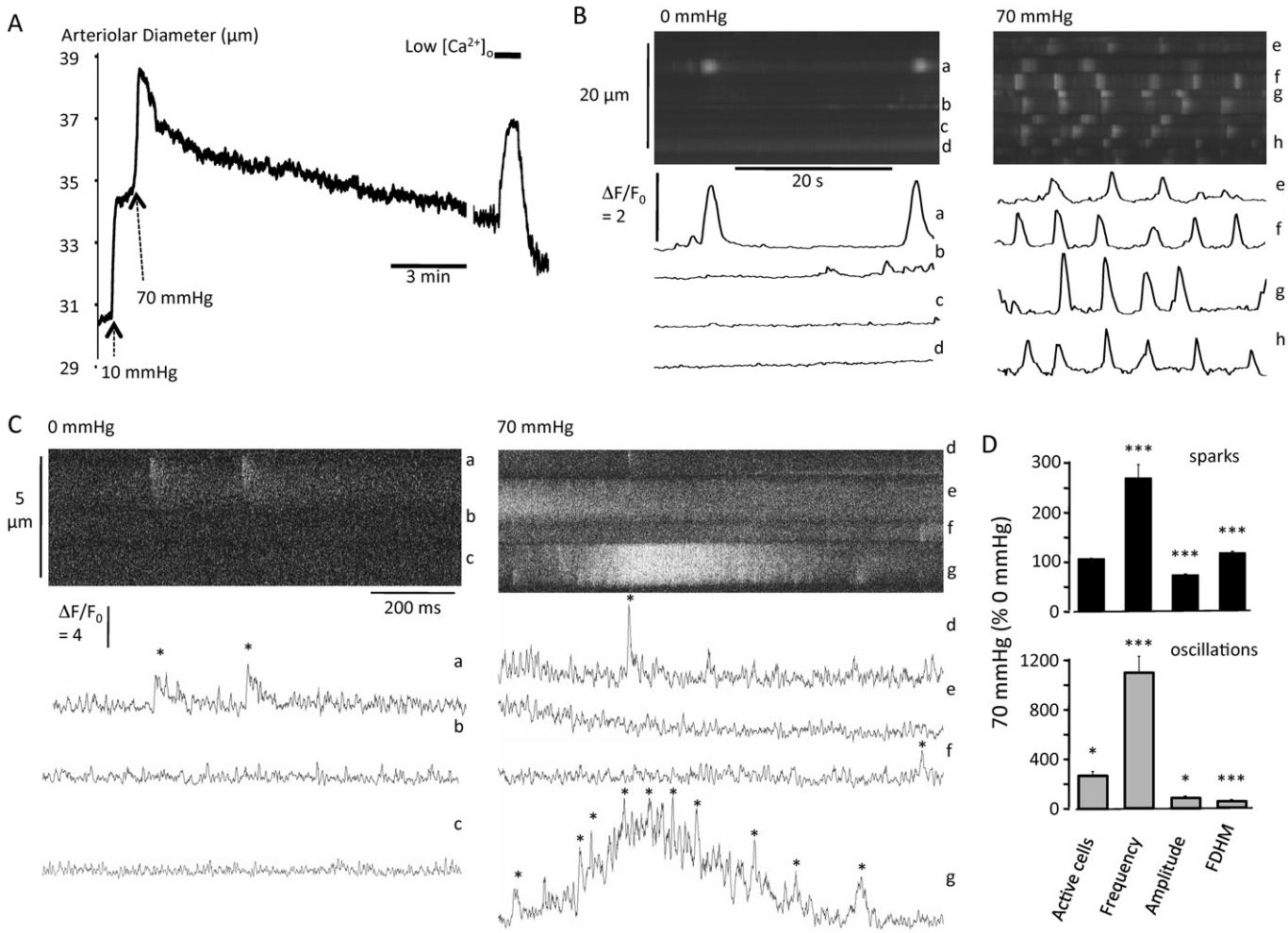

Figure 1

Myogenic tone was associated with an increased frequency of Ca^{2+} sparks and oscillations. (A) Pressure myograph plotting arteriolar diameter. This was extracted from phase-contrast images focussed on the plane of maximal diameter. Intraluminal pressure was stepped to 70 mmHg, leading to constriction. Removal of external Ca^{2+} led to reversible dilatation. (B) Line-scan images and time series plots showing changes in normalized fluorescence ($\Delta F/F_0$) for adjacent vascular myocytes (labelled 'a' to 'h') in two regions of the same vessel at 0 mmHg and after development of myogenic tone at 70 mmHg. The image was focussed on the smooth muscle layer in contact with the bottom of the recording chamber and the scan line was oriented transversely to the long axis of the smooth muscle cells. Ca^{2+} images were captured from different regions of the same arteriole before and after the diameter recordings in panel A. (C) High temporal resolution line scan images and plots for adjacent myocytes (labelled 'a' to 'g') demonstrate an increase in spark frequency associated with myogenic tone (* indicates spark). Sparks summated to generate an oscillation in cell 'g'. (D) Summary bar charts for spark and oscillation characteristics. Data recorded at 70 mmHg has been normalized to that at 0 mmHg in the same arterioles (54 cells in six arterioles from five animals). *** = $P < 0.001$, * = $P < 0.05$; versus 0 mmHg.

Data analysis

Analysis of the high speed $[Ca^{2+}]_c$ images was carried out offline. This required the identification and measurement of both brief Ca^{2+} sparks and relatively prolonged phasic increases in $[Ca^{2+}]$. It should be noted that, although the term 'oscillation' has been used to describe all prolonged elevations in $[Ca^{2+}]$ (>0.5 s), these cannot be distinguished from propagating Ca^{2+} waves in transverse line-scan recordings. 2D imaging suggests, however, that many of these prolonged events are actually Ca^{2+} waves (Stewart *et al.*, 2012). The time course of changes in F/F_0, spatially averaged over a ROI 5 pixels wide and centred on the site of maximal fluorescence, was plotted using ImageJ (Rasband, 1997–2011). Custom-designed software based on an 'à trous' wavelet transform was used to automate detection and analysis of Ca^{2+} sparks and oscillations, as previously described (Jeffries *et al.*, 2010). Spark and oscillation amplitude were defined as the maximum increase in $\Delta F/F_0$ for the ROI, while duration was estimated using the full duration at half-maximal fluorescence (FDHM) (Tumelty *et al.*, 2007).

Synchronization of Ca^{2+} oscillations in different vessels was assessed using the cross-correlation coefficient (CCC). Time series data for normalized fluorescence (F/F_0) were extracted from the Ca^{2+} line scan for each cell and exported into SPSS v18 for analysis. Periods in which there was no oscillatory activity or parallel changes in baseline were excluded from this analysis as they produce a spuriously high

CCC, unrelated to Ca^{2+} oscillations. CCC (r_{AB}) was calculated for each pair of contiguous cells (A and B) at zero lag using the expression:

$$r_{AB} = C_{AB}/S_A S_B$$

where C_{AB} is the time series cross-variance for cells A and B, S_A is the standard deviation for the time series for cell A and S_B is the standard deviation for the time series for cell B. The mean CCC for all the cell pairs in a vessel was calculated, and these values were compared with those in other vessels.

Relative changes in vessel resistance have been calculated based on the assumption that Poiseuille's law applies (i.e. that $R \propto 1/D^4$), where R is vessel resistance and D is vessel diameter (Krenz *et al.*, 1994). This will underestimate the actual change in resistance since the external arteriole diameter was recorded. This was necessary given the low level of optical contrast at the luminal margin of the endothelium, which made automated edge detection unreliable. Assuming an initial external diameter of 40 μm and a wall thickness of 5 μm, a 5% change in external diameter equates to a 32% change in resistance based on the estimated internal diameter, rather than 23% as calculated without this correction (McGahon *et al.*, 2007b). This correction has not been made within the results presented here.

Data from arterioles isolated from at least five different animals were used for each protocol described in the Results section. Summary data have been expressed as means ± SEM, and the statistical significance of apparent differences between means was assessed using the original, rather than the normalized data. Changes in arteriolar diameter and global $[Ca^{2+}]_c$ were tested using repeated measures ANOVA or paired *t*-test, as appropriate. We have previously shown that spark and oscillation data are not normally distributed, so non-parametric tests were used in these cases, i.e. the Wilcoxon signed-ranks test for paired data and the Mann–Whitney *U*-test for non-paired data (Tumelty *et al.*, 2007). In all cases, the accepted significance level was set at 0.05.

Results

Pressurized retinal arterioles generate myogenic tone in vitro

Pressurizing retinal arterioles to 70 mmHg led to myogenic tone development in 95% of vessels. In the example shown, this reduced the arteriolar diameter back to that observed at 10 mmHg (Figure 1A). Pressurization to 70 mmHg initially increased vessel diameter to 121.7 ± 2.8% of that at 0 mmHg, but this was followed by active constriction to a new steady-state value of 114.2 ± 2.7% ($P < 0.01$; $n = 10$). Assuming Poiseuille's law applies, myogenic tone increased vascular resistance on average by more than 45% relative to that immediately after the pressure step (see Methods). Removal of external Ca^{2+} caused a reversible dilatation, although this often failed to reach the maximum diameter immediately following pressurization (Figure 1A). Because of this, the latter measure was used as an estimate of passive diameter (see Figure 3 below).

Ca^{2+} sparks and oscillations are increased following myogenic tone development

Retinal arterioles were loaded with the Ca^{2+} indicator Fluo4, allowing pressure myography and Ca^{2+} imaging to be carried out in the same vessels (Figure 1B and C). Increasing intraluminal pressure to 70 mmHg induced myogenic constriction in 75% of these vessels. This constriction was similar in amplitude to that seen in the absence of Fluo4 (NS vs. unloaded vessels; $n = 6$). Ca^{2+} events were imaged before pressurization and then again after a new steady state had been achieved. Tone development was associated with clear increases in both spark and oscillation frequency (Figure 1D). Nearly all cells generated a small number of sparks even in unpressurized arterioles, so pressurization had little effect on the percentage of active cells, but mean spark frequency rose from 0.44 ± 0.05·per cell·s^{-1} at 0 mmHg to 1.17 ± 0.11·$cell^{-1}$·s^{-1} at 70 mmHg. Sparks were seen to summate, generating prolonged oscillations (Figure 1C). Oscillation frequency rose from 0.011 ± 0.003·per cell·s^{-1} at 0 mmHg to 0.118 ± 0.013·per cell·s^{-1} at 70 mmHg. This resulted both from a doubling in the number of cells generating Ca^{2+} oscillations and an increase in oscillation frequency within active cells (Figure 1D). Tone development was also associated with small reductions in spark and oscillation amplitude, an increase in spark duration and a reduction in oscillation duration (Figure 1D).

In 40% of vessels, myogenic tone was associated with phasic vasomotion (mean amplitude 1.2 ± 0.1 μm, mean frequency 17.1 ± 0.8·min^{-1}; Figure 2A). In these arterioles, Ca^{2+} oscillations in adjacent cells were well synchronized (Figure 2B). The CCC for Ca^{2+} signals was increased from 0.26 ± 0.05 in the absence of vasomotion to 0.57 ± 0.08 in its presence ($P < 0.02$; Figure 2C).

Ca^{2+} spark inhibitors dilate pressurized arterioles

In order to test the hypothesis that Ca^{2+} sparks play a constrictor role in retinal arterioles directly, we recorded diameter changes in pressurized vessels under experimental conditions known to inhibit Ca^{2+} sparks in retinal arteriolar myocytes (Tumelty *et al.*, 2007) (Figure 3 and Table 1). Tetracaine and ryanodine, which block ryanodine receptors and Ca^{2+} spark generation in vascular smooth muscle (Nelson *et al.*, 1995), resulted in dilatation. Inhibition of Ca^{2+} uptake into the sarcoplasmic reticulum (SR) using cyclopiazonic acid (CPA) produced a transient constriction followed by persistent dilatation. This correlated well with CPA's effects on Ca^{2+} sparks and oscillations in unpressurized retinal arterioles, with increased activity during the first 15–30 s after drug application followed by sustained inhibition (Tumelty *et al.*, 2007). Inhibition of L-type Ca^{2+} channels with nimodipine (Figure 3) also caused dilatation. The arteriolar diameter in the presence of each of the inhibitors tested was not significantly different from that measured immediately after pressurization to 70 mmHg. The dilatory effects of these agents were reversible and pressurized vessels re-constricted fully after a 5 min washout period. Mean diameters after washout, expressed as a percentage of the basal diameter after tone development and before drug addition, were 99.4 ± 0.6% (tetracaine), 100.5 ± 0.5% (ryanodine), 99.3 ± 0.2% (CPA)

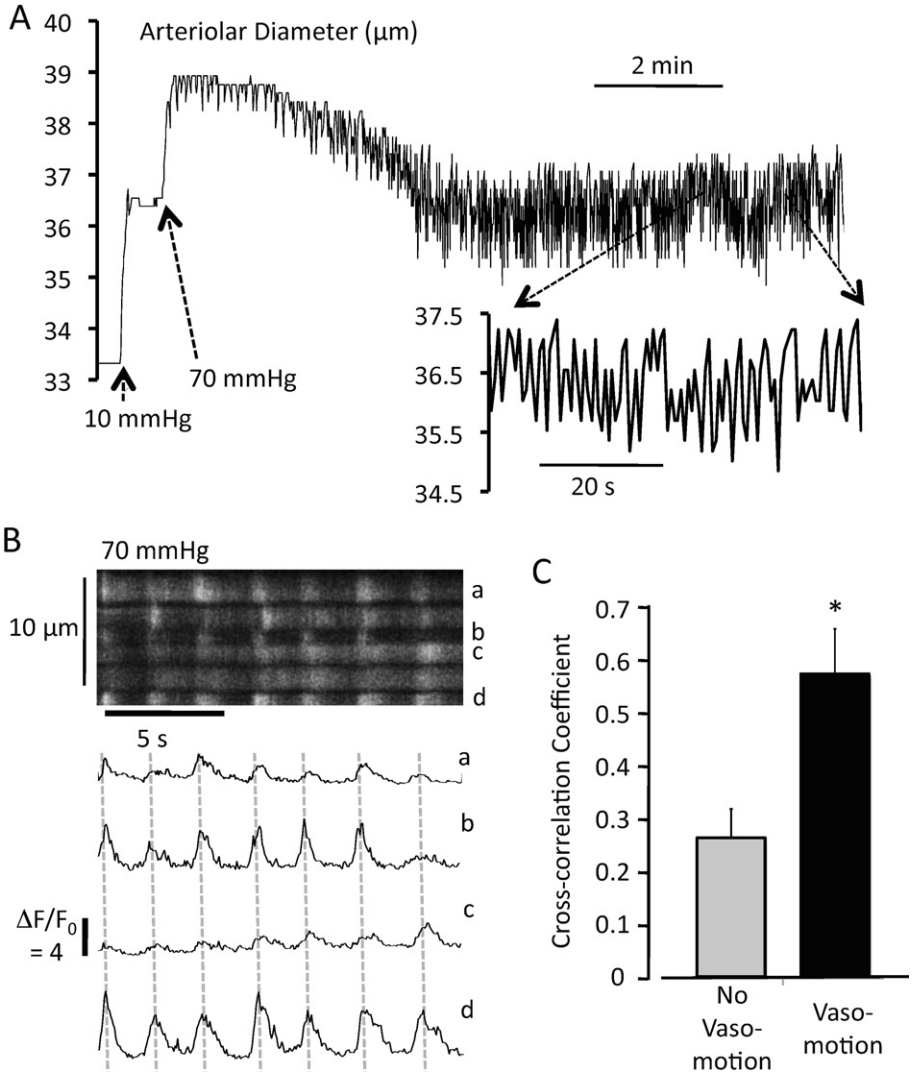

Figure 2

Vasomotion was associated with increased synchronization of Ca^{2+} oscillations. (A) Pressure myograph of diameter against time following step increases in pressure from 0 to 10 and then to 70 mmHg for an arteriole exhibiting vasomotion. A 1 min period (dashed arrows) has been plotted at higher resolution. (B) Confocal line-scan images and time series plots recorded after vasomotion was established in the arteriole in 'A'. Dashed lines indicate oscillation peaks for cell 'd'. (C) Summary data comparing cross correlation coefficients for Ca^{2+} line-scan data at 70 mmHg in arterioles exhibiting vasomotion with those that did not (32 cell pairs in six arterioles from five animals). * = $P < 0.05$, versus 'No vasomotion'.

Table 1

The effects of Ca^{2+} spark inhibitors on the diameters of pressurized retinal arterioles (mean ± SEM)

Diameters (μm):	Max diameter immediately following step to 70 mmHg	After steady-state tone development	Max diameter in presence of inhibitor
Ryanodine (n = 7)	39.7 ± 1.2	37.3 ± 1.6	40.0 ± 1.3**
Tetracaine (n = 5)	40.3 ± 1.5	38.9 ± 1.7	39.9 ± 1.5*
CPA (n = 9)	39.0 ± 1.2	36.7 ± 1.1	38.0 ± 0.9**
Nimodipine (n = 5)	33.3 ± 1.9	31.8 ± 1.9	33.6 ± 1.9*

*$P < 0.05$, **$P < 0.01$ versus steady-state tone; paired t-test.

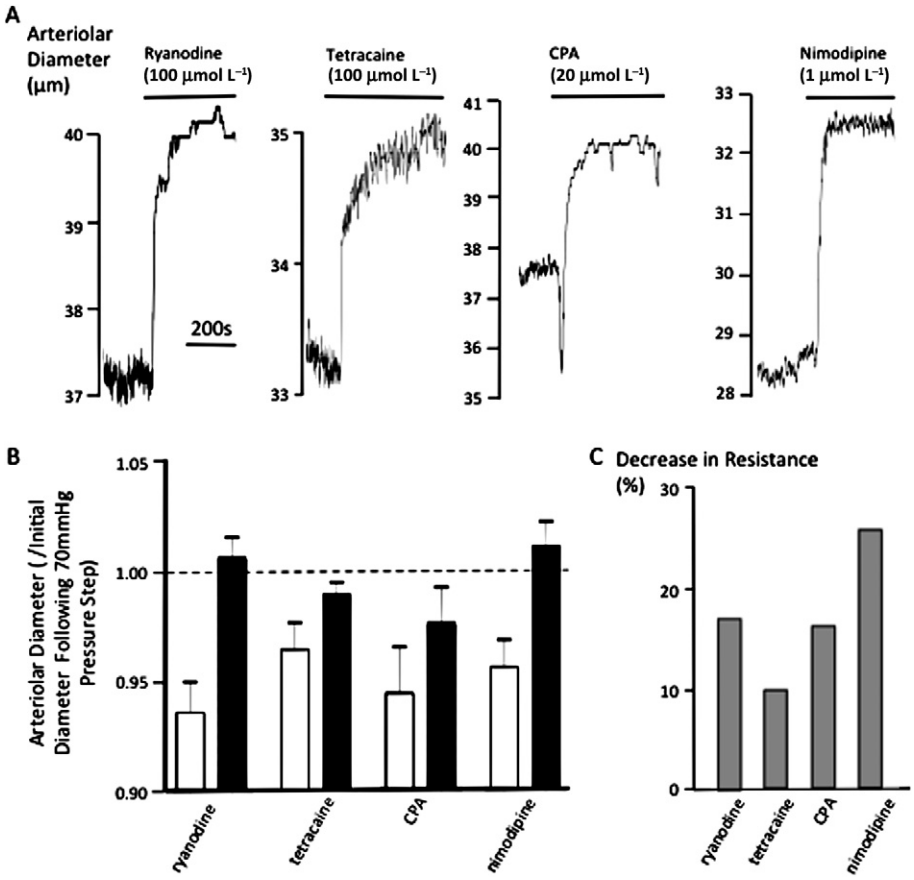

Figure 3

Inhibition of Ca^{2+} sparks relaxed arterioles exhibiting myogenic tone. (A) Changes in arteriole diameter at 70 mmHg. Each drug was superfused at the concentration indicated during the periods marked by a black bar. (B) Summary data from at least five vessels for the mean arteriolar diameter after tone generation at 70 mmHg both before (open columns) and during drug application (filled columns). All values have been normalized to the maximum (passive) diameter immediately following pressurization to 70 mmHg (represented by the dashed line). (C) Column chart indicating the calculated decrease in arteriolar resistance due to drug application.

and 97.8 ± 0.5% (nimodipine) (NS vs. basal diameter in each case).

Effects of cyclopiazonic acid on Ca^{2+} sparks and oscillations, mean $[Ca^{2+}]_c$ and vascular tone

As well as supporting an excitatory role for Ca^{2+} sparks, our observations suggest that, at the cellular level, development of myogenic tone is more dependent on phasic Ca^{2+} signals than tonic changes in mean $[Ca^{2+}]_c$ (Figure 2). This was tested further by comparing changes in spatially averaged $[Ca^{2+}]_c$ within vascular smooth muscle, as measured using Fura2 and microfluorimetry, with the frequency of Ca^{2+} sparks and oscillations under the same conditions. Myogenic tone was associated with an increase in $[Ca^{2+}]_c$ and high frequency of sparks and oscillations (Figures 1 and 4). Addition of CPA led to a further $[Ca^{2+}]_c$ rise and transient vasoconstriction. However, mean global $[Ca^{2+}]_c$ remained considerably elevated above baseline during the subsequent dilatation (Figure 4B). When CPA was applied to vessels loaded with Fluo4, it again produced a transient constriction (4.0 ± 1.0% reduction from diameter prior to drug application; $P < 0.01$) followed by dilatation (2.6 ± 0.5%; $P < 0.05$). This dilatation was associated with a dramatic reduction in Ca^{2+} sparks and oscillations (Figure 5). Under these conditions, therefore, tone correlated with Ca^{2+} spark and oscillation frequency, rather than global $[Ca^{2+}]_c$.

Discussion

The data presented above support the hypothesis that Ca^{2+} spark activity is excitatory in retinal arteriolar smooth muscle, promoting myogenic tone. Active constriction in response to increased intravascular pressure was associated with increases in spark and oscillation frequency (Figure 1). A similar study in cerebral arteries also found that spark and wave activity was increased following an increase in pressure (Jaggar, 2001). In that study, however, the use of ryanodine or thapsigargin to block spark and wave activity resulted in vasoconstriction, consistent with an inhibitory role for sparks. By contrast, interventions that have been shown to

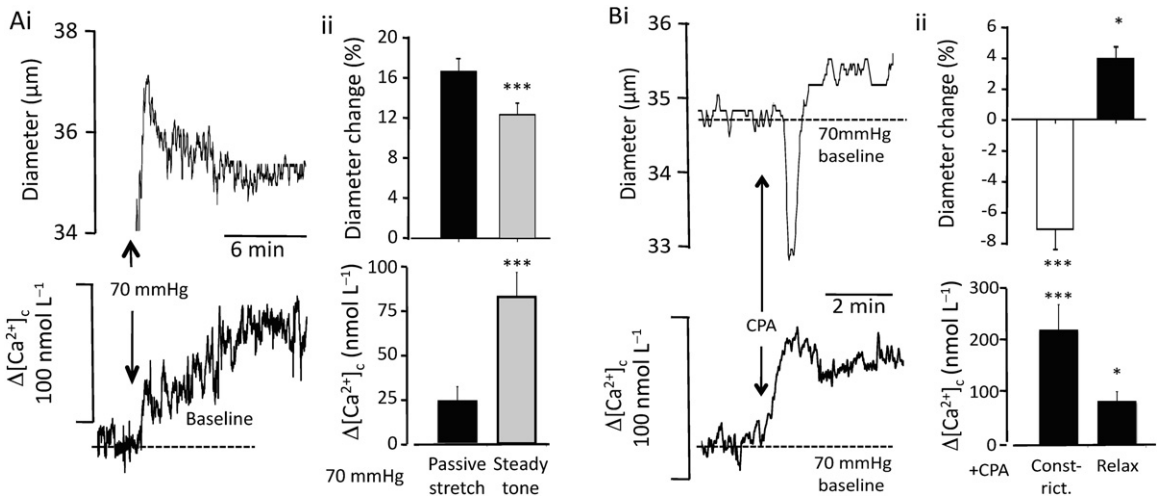

Figure 4

(A and B) Simultaneous recordings of diameter and $[Ca^{2+}]_c$ from arterioles loaded with Fura2. (Ai) Increasing intraluminal pressure from 0 to 70 mmHg resulted in myogenic constriction and an increase in global $[Ca^{2+}]_c$. (Aii) Summary data for changes in diameter and global $[Ca^{2+}]_c$ in response to pressurization to 70 mmHg (10 vessels from five animals). Values for the maximum diameter after the initial stretch and for the steady state after tone development are plotted separately. Diameter changes have been plotted as a percentage of the diameter at 0 mmHg (*** = $P < 0.001$ vs. 'passive stretch' at 70 mmHg). (Bi). Addition CPA (20 µmol·L^{-1}) led to brief constriction followed by sustained relaxation. $[Ca^{2+}]_c$ remained elevated throughout. (Bii) Summary data for CPA induced changes in diameter and global $[Ca^{2+}]_c$. Data for the transient constriction and the sustained relaxation are plotted separately. Diameter changes have been plotted as a percentage of the diameter at 70 mmHg prior to application of CPA (*** = $P < 0.001$ and * = $P < 0.05$ vs. baseline at 70 mmHg).

inhibit Ca^{2+} sparks in retinal arterioles produced a reversible dilatation (Figure 3), suggesting that spark activity plays a role in the maintenance of myogenic tone (Tumelty *et al.*, 2007). Mechanical responses to CPA were particularly interesting, with a brief constriction followed by maintained relaxation. This is consistent with previous studies of pressurized skeletal muscle arterioles (Kotecha and Hill, 2005) and fits well with our Ca^{2+} imaging data from unpressurized retinal arterioles, in which CPA produced a transient increase in sparks and oscillations followed by a persistent inhibition (Tumelty *et al.*, 2007). Spark inhibition during CPA-induced dilatation was also demonstrated directly in pressurized arterioles in the current study (Figure 5). Thapsigargin has also been used widely to inhibit SR Ca^{2+} uptake and spark activity (Nelson *et al.*, 1995; Jaggar, 2001). However, we found thapsigargin to be cytotoxic in our preparation, and so its effects could not be compared directly with those of CPA.

Overall, vascular tone was positively correlated with Ca^{2+} spark frequency under all conditions tested, presumably because sparks drive Ca^{2+} oscillations, which in turn lead to myocyte contraction. Others have shown that inhibition of either L-type Ca^{2+} channels or SR Ca^{2+} release alone does not completely reverse myogenic tone in skeletal muscle arterioles, but that this requires simultaneous inhibition of both pathways (Kotecha and Hill, 2005). In the current study, there were no statistically significant differences between the maximum diameters recorded immediately after pressurization and those observed following reversal of tone with individual blockers of SR Ca^{2+} release or Ca^{2+} influx (Figure 3). Incomplete dilatation cannot be ruled out from the relatively small data sets presented here, however, given the relatively small diameter changes seen in retinal arterioles as compared with those in other studies (Table 1). Kotecha and Hill (2005) also found that L-type Ca^{2+} channels make quite distinct contributions to the initiation and maintenance of arteriolar tone. This was not tested directly in our experiments.

One potential criticism of the current work is that the endothelium was present throughout, and so secondary effects due to endothelial signalling cannot be ruled out. We believe, however, that the dilator effects seen in response to pharmacological agents are more likely to be explained by direct effects on vascular smooth muscle. In previous studies, we have shown that there are no smooth muscle responses to endothelium dependent agents such as bradykinin and ACh when these are externally applied to this preparation. It is likely that this reflects limited access to the endothelium through the basement membrane and tight junctions of the blood–retinal barrier, as supported by the finding that the endothelium doesn't load with Ca^{2+} indicators applied to the outside of the isolated arterioles (Scholfield and Curtis, 2000). To date, our attempts to load the endothelium using intraluminal dye infusion have met with very limited success. It should also be remembered that the core hypothesis under test is that sparks in myocytes can contribute to myogenic tone development. Only Ca^{2+} events in the confocal image plane could be recorded, and this was set to include only the vascular smooth muscle layer (Figure 1). Our conclusion, therefore, that Ca^{2+} sparks in these cells play an excitatory role in myogenic tone in this vessel is independent of the upstream events responsible for their modulation. Overall, therefore, although we cannot exclude a contribution from the endothelium to the 'myogenic response' under these circumstances, it is unlikely to explain the drug-induced changes in response.

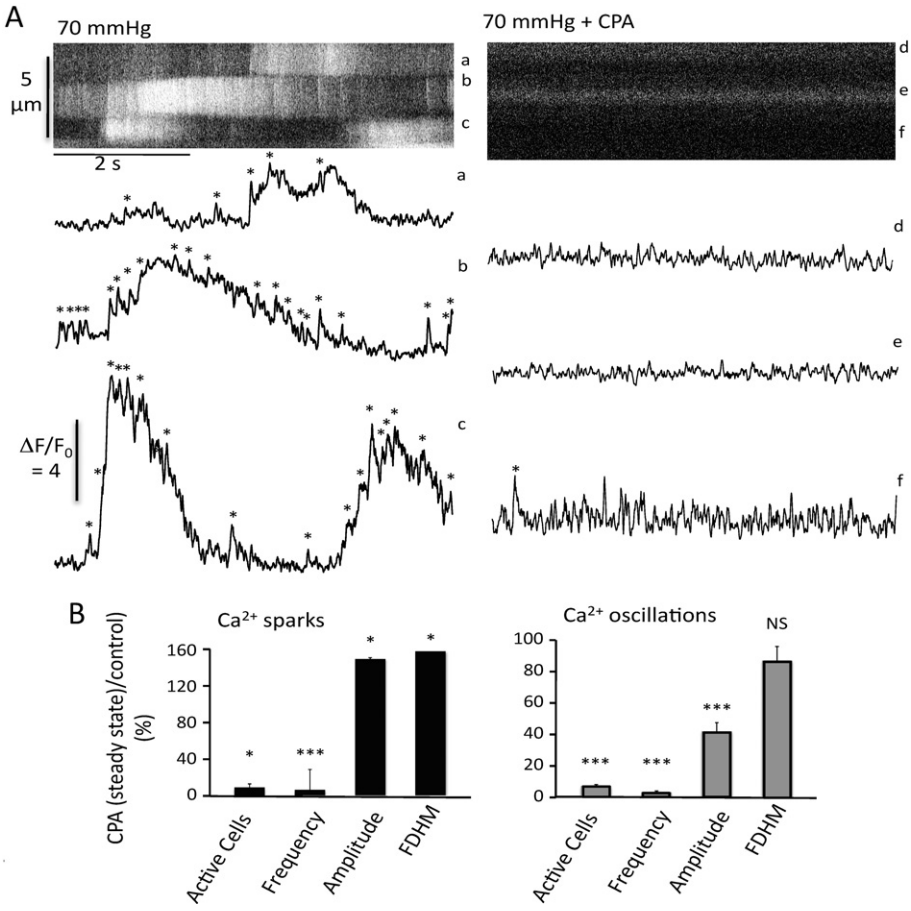

Figure 5

(A) Confocal Ca^{2+} images and time series data from a Fluo4-loaded arteriole pressurized to 70 mmHg before and during CPA-induced relaxation (* = Ca^{2+} sparks). (B) Summary data showing effects of CPA on Ca^{2+} sparks and oscillations (125 cells in nine arterioles in six animals). Parameters during CPA-induced relaxation have been normalized to values recorded in the same vessels at 70 mmHg prior to CPA application (*** = $P < 0.001$ and * = $P < 0.05$ vs. baseline at 70 mmHg).

A number of other studies suggest that RyRs can play an excitatory role within vascular smooth muscle. Pharmacological inhibition of RyR activity reduces depolarization induced increases in global Ca^{2+} in isolated afferent renal arterioles (Fellner and Arendshorst, 2007). Genetic and pharmacological interventions likely to reduce RyR open probability *in vivo* increased basal renal blood flow and inhibited agonist and L-type Ca^{2+}-channel-mediated constrictor responses (Thai *et al.*, 2007). Consistent with this, mechanical stretch applied to isolated afferent arteriolar smooth muscle cells elicited an integrin-dependent increase in spark frequency and global $[Ca^{2+}]_c$ (Balasubramanian *et al.*, 2007). Ca^{2+} imaging of smooth muscle cells isolated from the portal vein revealed the presence of specific sites at which the probability of spontaneous spark activity was much higher than elsewhere (Bolton and Gordienko, 1998). Subsequent experiments showed that propagating Ca^{2+} waves driving cell contraction were often initiated from these 'frequent-discharge sites', suggesting an excitatory role for sparks (Gordienko *et al.*, 2001). Such reports contrast, however, with findings in systemic arteries, in which spark inhibition causes constriction (Nelson *et al.*, 1995; Cheng and Lederer, 2008; Westcott *et al.*, 2012). This has led to the generally accepted model proposing that sparks relax vascular smooth muscle through BK activation, hyperpolarization and Ca^{2+} channel deactivation (Nelson *et al.*, 1995; Cheng and Lederer, 2008).

It is tempting to propose that the apparently contrasting roles for sparks in retinal arterioles and larger arteries reflect differences in signalling strategies for different sizes of vessel in the vascular tree. It has been shown, for example, that whereas the smooth muscle in feed arteries in skeletal muscle display sparks and waves, sparks were not seen in pressurized arterioles. Inhibition of ryanodine receptors blocked sparks and waves in the arteries but increased myogenic tone, while the same blockers had no effect on either Ca^{2+} signalling or diameter in arterioles (Westcott and Jackson, 2011; Westcott *et al.*, 2012). However, other recent papers have shown that sparks can also play an inhibitory role in pressurized cerebral arterioles, in which acidosis was shown to inhibit Ca^{2+} waves but promote Ca^{2+} sparks (Dabertrand *et al.*, 2012). Acidosis-dependent vasodilatation was substantially reduced by pharmacological inhibition of sparks or BK currents. In a separate report, hydrogen sulphide dependent vasodilatation in cerebral arterioles was correlated with an increased frequency of

Ca^{2+} sparks and transient BK currents, again consistent with an inhibitory role (Liang *et al.*, 2012). The present study suggests yet another variation on this theme, with Ca^{2+} sparks being observed within pressurized arterioles but apparently playing an excitatory, rather than an inhibitory role. Other studies in skeletal muscle arterioles have failed to demonstrate Ca^{2+} spark activity, even under conditions in which sparks were routinely observed in cerebral vessels (Yang *et al.*, 2009; Westcott and Jackson, 2011; Westcott *et al.*, 2012). Taken together, these findings indicate considerable regional heterogeneity both within and between vascular beds.

Our failure to demonstrate an inhibitory action of sparks could be explained if functional BK channels were not expressed in the relevant myocytes, since BK activation by sparks is a key step in their vasodilator actions (Cheng and Lederer, 2008). However, we have recorded classical 'spontaneous transient outward' BK currents from retinal arteriolar smooth muscle and demonstrated that their inhibition constricts pressurized retinal arterioles *in vitro* (McGahon *et al.*, 2007a). *In vivo* experiments have also shown that BK channel activation causes retinal vasodilatation in rats and that ACh-induced vasodilatation is reduced by BK channel inhibition (Mori *et al.*, 2011a,b). These findings suggest that BK currents are expressed in retinal arteriolar smooth muscle, and that BK activation favours dilatation in the retinal vasculature. Nevertheless, the dominant effect of Ca^{2+} sparks in retinal arterioles, as revealed by direct observation with high-speed Ca^{2+} imaging, appears to be excitatory under conditions of myogenic tone. We have previously reported similar results in unpressurized arterioles both under control conditions and in the presence of constrictor agonists (Jeffries *et al.*, 2010; Tumelty *et al.*, 2011). If sparks exerted a negative feedback effect by opening BK channels, one would expect spark inhibitors to produce further constriction and not dilatation as described here (Figure 3). There is growing evidence in the literature for heterogeneity in BK function, with a range of potential activators and inhibitors interacting to determine the overall level of BK activity within smooth muscle in any given vascular bed (see review Hill *et al.*, 2010). Identifying the cell mechanisms that determine whether sparks activate BK channels, resulting in vasodilatation, or summate to generate more prolonged, global Ca^{2+} waves and oscillations, leading to constriction, remains an important goal for future research.

Following pressurization, the spatially averaged global $[Ca^{2+}]_c$, as recorded using Fura2, increased as myogenic tone developed (Figure 4A). The qualitative divergence between changes in mean $[Ca^{2+}]_c$ and spark and oscillation frequency during CPA treatment provided a direct test of their relative significance in determining tone. In CPA-treated retinal arterioles, relaxation was associated with an elevated average $[Ca^{2+}]_c$ across the tissue as a whole but with a reduction in Ca^{2+} sparks and oscillations (Figure 5). We do not believe that the increased average $[Ca^{2+}]_c$ reflected any contribution to the signal from endothelial cells since, as already noted, the endothelium does not load with Fura2 when applied to the outside of retinal arterioles (Scholfield and Curtis, 2000). This suggests that vascular tone is determined by changes in the frequency of phasic changes in global $[Ca^{2+}]_c$ within individual smooth muscle cells rather than the overall average within the tissue as a whole (Sanderson *et al.*, 2010). This is not meant to imply that global $[Ca^{2+}]_c$ changes play no role in excitation–contraction coupling, but rather that the tissue-averaged Fura2 signal does not reflect the signal driving contraction in any individual cell. Synchronization of Ca^{2+} oscillations within the tissue was associated with vasomotion but, as reported in cerebral arteries, synchronization was not required to increase tone (Figure 2) (Mufti *et al.*, 2010). The functional benefits of frequency-modulated Ca^{2+} signalling remain unclear, but similar patterns have been observed in other vascular smooth muscles, both in response to increased transmural pressure and constrictor agonists (Perez and Sanderson, 2005; Mufti *et al.*, 2010). It seems, therefore, that this may be a preferred signalling mode, even in what are classically regarded as tonically contractile tissues.

The results reported here focus on the role of RyR-dependent Ca^{2+} sparks in the generation of Ca^{2+} oscillations and the development of myogenic tone in pressurized retinal arterioles, without considering other mechanisms involved. Inositol 1,4,5-triphosphate receptors (IP_3Rs) have recently been shown to contribute to Ca^{2+} waves and myogenic tone in both arteries and arterioles supplying the cremasteric muscle (Westcott *et al.*, 2012). A contribution by IP_3Rs to myogenic responses in retinal arterioles has not been tested for directly here and cannot be ruled out. The observation that nimodipine dilates these vessels (Figure 3) is consistent with studies in skeletal muscle arterioles, showing that increased intraluminal pressure results in depolarization of the vascular smooth muscle, as this would be expected to activate Ca^{2+} influx through voltage operated Ca^{2+} channels. In cremasteric arterioles, development of myogenic tone is completely prevented by nifedipine, another L-type Ca^{2+} channel inhibitor, but once tone is established it is only partially reversed by the same agent. This suggests that L-type channels play an important, if complex, role and that different mechanisms may be involved in the generation and maintenance of tone (Kotecha and Hill, 2005). The underlying stretch sensor responsible for the depolarization is even less well understood but may involve stretch activated channels of the TRP superfamily (for review, see Lim *et al.*, 2012). Other myogenic mechanisms may not generate increases in $[Ca^{2+}]_c$ but may augment or sustain tone through sensitization of the contractile machinery to Ca^{2+}, e.g. in response to activation of PKC or the RhoA/Rho kinase pathway, or generation of reactive oxygen species (Schubert *et al.*, 2008). The upstream signalling molecules implicated in this process are diverse and will not be considered further here. This diversity, however, underscores the mechanistic complexity underpinning pressure-induced myogenic constriction.

In conclusion, we have demonstrated that Ca^{2+} sparks have an excitatory function in pressurized retinal arterioles, promoting the generation of Ca^{2+} waves and vasoconstriction. This contrasts with many previous studies on vascular smooth muscle under conditions of myogenic tone, which have demonstrated an inhibitory role for sparks. It suggests that Ca^{2+} signalling may show an even greater complexity than previously assumed, since it appears that localized Ca^{2+} release events can play more than one role, even within a single tissue type. We have also shown that in the presence of the SR Ca^{2+} uptake inhibitor CPA, vasodilatation was associated with a decrease in spark and wave frequency, even though mean global $[Ca^{2+}]_c$ increased. This suggests that

phasic Ca^{2+} signalling plays an important role in the regulation of contractile activity in vascular smooth muscle, with the degree of intercellular synchronization determining whether the resulting mechanical activity is tonic or phasic.

Conflict of interest

No conflict of interest exists for any of the authors.

References

Balasubramanian L, Ahmed A, Lo C-M, Sham JSK, Yip K-P (2007). Integrin-mediated mechanotransduction in renal vascular smooth muscle cells: activation of calcium sparks. Am J Physiol Regul Integr Comp Physiol 293: R1586–R1594.

Bolton T, Gordienko D (1998). Confocal imaging of calcium release events in single smooth muscle cells. Acta Physiol Scand 164: 567–575.

Burdyga T, Wray S (2005). Action potential refractory period in ureter smooth muscle is set by Ca sparks and BK channels. Nature 436: 559–562.

Cheng H, Lederer WJ (2008). Calcium sparks. Physiol Rev 88: 1491–1545.

Cheng H, Lederer WJ, Cannell MB (1993). Calcium sparks: elementary events underlying excitation-contraction coupling in heart muscle. Science 262: 740–744.

Curtis TM, Tumelty J, Dawicki J, Scholfield CN, McGeown JG (2004). Identification and spatiotemporal characterization of spontaneous Ca2+ sparks and global Ca2+ oscillations in retinal arteriolar smooth muscle cells. Invest Ophthalmol Vis Sci 45: 4409–4414.

Dabertrand F, Nelson MT, Brayden JE (2012). Acidosis dilates brain parenchymal arterioles by conversion of calcium waves to sparks to activate BK channels/novelty and significance. Circ Res 110: 285–294.

Fellner SK, Arendshorst WJ (2007). Voltage-gated Ca2+ entry and ryanodine receptor Ca2+-induced Ca2+ release in preglomerular arterioles. Am J Physiol Renal Physiol 292: F1568–F1572.

Gordienko DV, Greenwood IA, Bolton TB (2001). Direct visualization of sarcoplasmic reticulum regions discharging Ca2+sparks in vascular myocytes. Cell Calcium 29: 13–28.

Grynkiewicz G, Poenie M, Tsien RY (1985). A new generation of Ca2+ indicators with greatly improved fluorescence properties. J Biol Chem 260: 3440–3450.

Hill MA, Sun Z, Martinez-Lemus L, Meininger GA (2007). New technologies for dissecting the arteriolar myogenic response. Trends Pharmacol Sci 28: 308–315.

Hill MA, Yang Y, Ella SR, Davis MJ, Braun AP (2010). Large conductance, Ca2+-activated K+ channels (BKCa) and arteriolar myogenic signaling. FEBS Lett 584: 2033–2042.

Iino M, Kasai H, Yamazawa T (1994). Visualization of neural control of intracellular Ca2+ concentration in single vascular smooth muscle cells in situ. EMBO J 13: 5026–5031.

Jaggar JH (2001). Intravascular pressure regulates local and global Ca2+ signaling in cerebral artery smooth muscle cells. Am J Physiol Cell Physiol 281: C439–C448.

Jeffries O, McGahon MK, Bankhead P, Lozano MM, Scholfield CN, Curtis TM *et al.* (2010). cAMP/PKA-dependent increases in Ca Sparks, oscillations and SR Ca stores in retinal arteriolar myocytes after exposure to vasopressin. Invest Ophthalmol Vis Sci 51: 1591–1598.

Kilkenny C, Browne W, Cuthill IC, Emerson M, Altman DG (2010). NC3Rs Reporting Guidelines Working Group. Br J Pharmacol 160: 1577–1579.

Kotecha N, Hill MA (2005). Myogenic contraction in rat skeletal muscle arterioles: smooth muscle membrane potential and Ca2+ signaling. Am J Physiol Heart Circ Physiol 289: H1326–H1334.

Krenz GS, Lin J, Dawson CA, Linehan JH (1994). Impact of parallel heterogeneity on a continuum model of the pulmonary arterial tree. J Appl Physiol 77: 660–670.

Liang GH, Xi Q, Leffler CW, Jaggar JH (2012). Hydrogen sulfide activates Ca2+ sparks to induce cerebral arteriole dilation. J Physiol 590: 2709–2720.

Lim M, Choi S-K, Cho Y-E, Yeon S-I, Kim E-C, Ahn D-S *et al.* (2012). The role of sphingosine kinase 1/sphingosine-1-phosphate pathway in the myogenic tone of posterior cerebral arteries. PLoS ONE 7: e35177.

McGahon MK, Dash DP, Arora A, Wall N, Dawicki J, Simpson DA *et al.* (2007a). Diabetes downregulates large-conductance Ca2+-activated potassium beta 1 channel subunit in retinal arteriolar smooth muscle. Circ Res 100: 703–711.

McGahon MK, Dawicki JM, Arora A, Simpson DA, Gardiner TA, Stitt AW *et al.* (2007b). Kv1.5 is a major component underlying the A-type potassium current in retinal arteriolar smooth muscle. Am J Physiol Heart Circ Physiol 292: H1001–H1008.

McGeown JG (2010). Seeing is believing! Imaging Ca2+-signalling events in living cells. Exp Physiol 95: 1049–1060.

McGrath J, Drummond G, Kilkenny C, Wainwright C (2010). Guidelines for reporting experiments involving animals: the ARRIVE guidelines. Br J Pharmacol 160: 1573–1576.

Mandala M, Heppner TJ, Bonev AD, Nelson MT (2007). Effect of endogenous and exogenous nitric oxide on calcium sparks as targets for vasodilation in rat cerebral artery. Nitric Oxide 16: 104–109.

Marchand A, Abi-Gerges A, Saliba Y, Merlet E, Lompre AM (2012). Calcium signaling in vascular smooth muscle cells: from physiology to pathology. Adv Exp Med Biol 740: 795–810.

Martinez-Lemus LA (2012). The dynamic structure of arterioles. Basic Clin Pharmacol Toxicol 110: 5–11.

Mori A, Suzuki S, Sakamoto K, Nakahara T, Ishii K (2011a). BMS-191011, an opener of large-conductance Ca2+-activated potassium channels, dilates rat retinal arterioles in vivo. Biol Pharm Bull 34: 150–152.

Mori A, Suzuki S, Sakamoto K, Nakahara T, Ishii K (2011b). Role of calcium-activated potassium channels in acetylcholine-induced vasodilation of rat retinal arterioles in vivo. Naunyn Schmiedebergs Arch Pharmacol 383: 27–34.

Mufti RE, Brett SE, Tran CHT, Abd El-Rahman R, Anfinogenova Y, El-Yazbi A *et al.* (2010). Intravascular pressure augments cerebral arterial constriction by inducing voltage-insensitive Ca2+ waves. J Physiol 588: 3983–4005.

Nelson MT, Cheng H, Rubart M, Santana LF, Bonev AD, Knot HJ *et al.* (1995). Relaxation of arterial smooth muscle by calcium sparks. Science 270: 633–637.

Perez JF, Sanderson MJ (2005). The contraction of smooth muscle cells of intrapulmonary arterioles is determined by the frequency of Ca2+ oscillations induced by 5-HT and KCl. J Gen Physiol 125: 555–567.

Rasband WS (1997–2011). Image J. National Institutes of Health: Bethesda, MD.

Sanderson MJ, Bai Y, Perez-Zoghbi J (2010). Ca(2+) oscillations regulate contraction of intrapulmonary smooth muscle cells. Adv Exp Med Biol 661: 77–96.

Sato K, Ozaki H, Karaki H (1988). Changes in cytosolic calcium level in vascular smooth muscle strip measured simultaneously with contraction using fluorescent calcium indicator fura 2. J Pharmacol Exp Ther 246: 294–300.

Scholfield CN, Curtis TM (2000). Heterogeneity in cytosolic calcium regulation among different microvascular smooth muscle cells of the rat retina. Microvasc Res 59: 233–242.

Schubert R, Lidington D, Bolz S-S (2008). The emerging role of Ca2+ sensitivity regulation in promoting myogenic vasoconstriction. Cardiovasc Res 77: 8–18.

Secomb TW (2008). Theoretical models for regulation of blood flow. Microcirculation 15: 765–775.

Stewart M, Needham M, Bankhead P, Gardiner TA, Scholfield CN, Curtis TM *et al.* (2012). Feedback via Ca2+-activated ion channels modulates endothelin1 signalling in retinal arteriolar smooth muscle. Invest Ophthalmol Vis Sci 53: 3059–3066.

Thai TL, Fellner SK, Arendshorst WJ (2007). ADP-ribosyl cyclase and ryanodine receptor activity contribute to basal renal vasomotor tone and agonist-induced renal vasoconstriction in vivo. Am J Physiol Renal Physiol 293: F1107–F1114.

Tumelty J, Scholfield N, Stewart M, Curtis T, McGeown G (2007). Ca2+-sparks constitute elementary building blocks for global Ca2+-signals in myocytes of retinal arterioles. Cell Calcium 41: 451–466.

Tumelty J, Hinds K, Bankhead P, McGeown NJ, Scholfield CN, Curtis TM *et al.* (2011). Endothelin 1 stimulates Ca2+-sparks and oscillations in retinal arteriolar myocytes via IP3R and RyR-dependent Ca2+ release. Invest Ophthalmol Vis Sci 52: 3874–3879.

Westcott EB, Jackson WF (2011). Heterogeneous function of ryanodine receptors, but not IP3 receptors, in hamster cremaster muscle feed arteries and arterioles. Am J Physiol Heart Circ Physiol 300: H1616–H1630.

Westcott EB, Goodwin EL, Segal SS, Jackson WF (2012). Function and expression of ryanodine receptors and inositol 1,4,5-trisphosphate receptors in smooth muscle cells of murine feed arteries and arterioles. J Physiol 590: 1849–1869.

Yang Y, Murphy TV, Ella SR, Grayson TH, Haddock R, Hwang YT *et al.* (2009). Heterogeneity in function of small artery smooth muscle BKCa: involvement of the β1-subunit. J Physiol 587: 3025–3044.

Zhuge R, Fogarty KE, Baker SP, McCarron JG, Tuft RA, Lifshitz LM *et al.* (2004). Ca(2+) spark sites in smooth muscle cells are numerous and differ in number of ryanodine receptors, large-conductance K(+) channels, and coupling ratio between them. Am J Physiol Cell Physiol 287: C1577–C1588.